Chinese Chemical Letters 31 (2020) 2115–2118

Contents lists available at ScienceDirect

Chinese Chemical Letters

journal homepage: www.elsevier.com/locate/cclet

Communication

RhIr@MoS_2 nanohybrids based disposable microsensor for the point-of-care testing of NADH in real human serum

Dongqing Ji[a,b], Zi Ying[a], Yuan Zhang[a,b,*], Wei Chen[c], Metini Janyasupab[d], Xinghua Gao[a], Lingyan Feng[a,*], Weijia Wen[a]

[a] Materials Genome Institute, Shanghai University, Shanghai 200444, China
[b] State Key Laboratory of Transducer Technology, Shanghai Institute of Microsystem and Information Technology, Chinese Academy of Sciences, Shanghai 200050, China
[c] Department of Emergency, Tongji Hospital, Tongji University School of Medicine, Shanghai 200065, China
[d] Department of Electronics Engineering, King Mongkut's Institute of Technology Ladkrabang, Bangkok 10520, Thailand

ARTICLE INFO

Article history:
Received 17 November 2019
Received in revised form 17 December 2019
Accepted 19 December 2019
Available online 20 December 2019

Keywords:
MoS_2
Nanohybrid
Electrochemical microsensor
Point-of-care (POC) test
Cancer diagnosis

ABSTRACT

Dihydronicotinamide adenine dinucleotide (NADH) is an important enzyme in all living cells, which is found to be abnormally expressed in cancer cells. Since it is redox-active, an electrochemical detection method would be suitable for monitoring its concentration in biological fluids. Here we present a strategy for specific determination of NADH in real human serum by using RhIr@MoS_2 nanohybrids based microsensor. To implement the protocol, RhIr nanocrysrals are *in-situ* grown onto MoS_2 interlayers forming a nanohybrid structure (RhIr@MoS_2). After being locally deposited on an electrochemical microsensor, it could be used for the analysis of NADH. The developed RhIr@MoS_2 nanohybrids based microsensor possesses the ability for analyzing NADH at the applied potential of 0.07 V (much lower than most reported values). The detection limit is evaluated as low as 1 nmol/L even in bovine serum albumin (BSA) media. In addition, the sampling analysis of human serum from cancer patients and health controls shows that the microsensor displays good diagnostic sensitivity and specificity, illustrating that this developed detection technique is a relatively accurate method for measuring NADH in biological fluids. The proposed electrochemical microsensor assay also owns the benefits of convenience, disposable and easy processing, which make it a great possibility for future point-of-care cancer diagnosis.

Dihydronicotinamide adenine dinucleotide (NADH) is an important enzyme found in all living cells, and its expression is related to reactive oxygen species (ROS) including O_2^- and H_2O_2 [1]. It has been reported that ROS regulates mitochondrial redox metabolism, and the intracellular NADH levels would be declined with elevating H_2O_2 concentration [2,3]. The previous discussion indicates that H_2O_2 is overexpressed in cancer cells [4,5]. The generated H_2O_2 can cause the depletion of intracellular NADH resulting in lower concentration of NADH in cancer cells than that in normal cells. Therefore, the monitoring of NADH levels in real human blood is promising for cancer patients to be quickly screened for metastasis or recurrence and may longer life expectancy.

The detection of NADH is mostly focused on fluorescence assay and electrochemical sensors [6–8]. Between these two methods, the electrochemical measurement of NADH is the predominating method and has received considerable interest due to the redox-activity of NADH [9–11]. Besides, it is difficult to distinguish between NADH and reduced nicotinamide adenine dinucleotide phosphate (NADPH) by using fluorescence, as they have similar fluorescent properties [12,13]. Accordingly, electrochemical detection would be suitable for the analysis of NADH. Electrochemical sensors also have the the advantages of economy, design flexibility and ease for realizing the miniaturization and the integration, and are expected to speed up the transition towards point-of-care diagnostic devices [14–16]. However, the major challenge for electrochemical sensing of NADH is about the high overpotential for measurements [17]. Although NADH is a redox-active molecule, the oxidation of NADH is highly irreversible and requires considerable overpotential, even up to 1 V at a bare metal electrode. The use of such a high overpotential leads to the fouling of electrodes and may suffer from interference [18].

* Corresponding authors at: Materials Genome Institute, Shanghai University, Shanghai 200444, China.
E-mail addresses: zhangyuan@shu.edu.cn (Y. Zhang), lingyanfeng@t.shu.edu.cn (L. Feng).

https://doi.org/10.1016/j.cclet.2019.12.029
1001-8417/

To address these problems, new sensing materials with multi-functions should be explored.

Graphene- like molybdenum disulfide (MoS_2) is a two-dimensional (2D) semiconductor with similar ultrathin layered structure to graphene, and exhibits fine properties that depend on the number of layers [19,20]. With interesting indirect-to-direct bandgap transition for MoS_2 material from bulk to ultrathin structure, it owns the ability to provide the high performance for an electrochemical sensor system [21]. However, the ultrathin MoS_2 becomes less stable in its freestanding state, and would re-stack together. Therefore, it needs to incorporate hetero-species into MoS_2 interlayers to generate a new 3D architecture [22]. Metal nanomaterial is a good candidate, which is not limited to be a strut between MoS_2 layers but also a catalyst facilitating the reactions [23,24].

Herein, we propose the use of RhIr alloy nanocrystals *in-situ* incorporation into ultra-thin MoS_2 interlayers (defined as RhIr@-MoS_2 nanohybrid) not only to achieve structure controllable but also to be responsible for catalyzing interfacial charge-transfer and mass diffusion processes. Then, the developed RhIr@MoS_2 nanohybrids are locally deposited onto screen printed sensor platform to construct a disposable microsensor for NADH determination.

The ultra-thin 2D MoS_2 used in this work was prepared by solvent exfoliation approach. After incorporation of RhIr nanocrystals onto MoS_2, a typical transmission electron microscopy (TEM) image (Fig. 1a) shows that all the *in-situ* obtained nanocrystals are well dispersed on the whole area of 2D MoS_2, and no particle is dissociated in the observation region. The selected-area electron diffraction (SAED) image shown in inset of Fig. 1a is comprised with hexagonal diffraction spots and polycrystalline diffraction pattern. The typical hexagonal diffraction pattern is obtained from the single-crystal MoS_2 domain, while the diffracted image of polycrystalline taken in the diffraction system is composed of a superposition of many small-sized RhIr domains. The scanning transmission electron microscopy (STEM) combined with energy dispersive X-ray spectrometry (EDS) analysis (Fig. 1b) reveals the elemental composition of RhIr@MoS_2 nanohybrids. From the compositional line profiles, it could be seen that Rh, Ir, Mo and S signals are obtained through the line drawn across the sample. Among them, Mo and S atoms come from layered MoS_2 material, and Rh and Ir atoms belong to the introduced RhIr nanocrystals. Both Rh and Ir lines have the maximum concentration at the particles' region. In addition, the similar line profiles obtained from Rh and Ir reveal a homogeneous distribution of Rh and Ir atoms in the nanocrystals. All of the results demonstrate that the RhIr alloy nanocrystals are successfully deposited onto MoS_2 surface.

In the synthesis of RhIr@MoS_2 nanohybrids, there are also several knacks in particular need attention. Firstly, the concentration of metal precursors has considerable influence on the density and distribution of RhIr nanocrystals in final nanohybrids. With the increasing of metal precursors, there are more and more nanocrystals formed on MoS_2 surface (Figs. S1a-c in Supporting information). In addition, the reaction time for producing RhIr nanocrystals should be strictly controlled. Under a long reaction time (about 30 min), RhIr nanoaggregates with the diameter of about 40−50 nm are obtained, which is hard to anchor on the surface of MoS_2 (Fig. S1d in Supporting information). Furthermore, the oleylamine synthesis strategy is chose for preparation of RhIr@MoS_2 nanohybrids in this work. Oleylamine used in the synthesis is not only for the preparation of RhIr, but also for the stabilization of ultra-thin layered MoS_2 [25]. Before the formation of RhIr nanocrystals, MoS_2 is firstly covered by a protective coating of oleylamine that stabilizes the suspension, avoiding aggregation and oxidation phenomena. Then, the synthesized RhIr nanocrystals could be easily deposited onto MoS_2 surface forming nanohybrid structure.

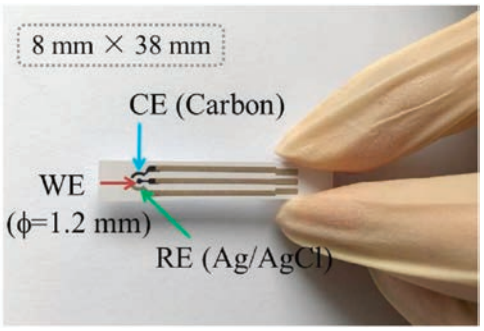

Fig. 2. Microsensor propotype fabricated by screen-printing technology (WE: working electrode, CE: counter electrode and RE: reference electrode).

After the RhIr@MoS_2 nanohybrids with desired distribution and morphology being produced, an electrochemical microsensor is equipped and employed for NADH analysis. Fig. 2 displays the configuration of designed microsensor, which is composed with a three-electrode system, *i.e.,* working, counter and reference electrode. Three of the electrodes are screen printed on a polyethylene terephalate (PET) substrate. The dimension of single sensor is 8 mm × 38 mm, and the diameter of working electrode is 1.2 mm. The widths of both reference and counter electrodes shown as two arcs in microsensor configuration are 0.7 mm. The distances between working electrode and the two other electrodes are 0.6 mm. The center-to-center spacing between each two conducting wires is 2 mm. The counter electrode is printed with carbon ink, and reference electrode is printed with Ag/AgCl ink. With the assistance of an ink-jet printer, the prepared RhIr@MoS_2 hybrid sensing material is locally deposited onto the screen printed microsensor platform. Therefore, the relatively low manufacturing cost can make single-use and disposable microsensors a reality.

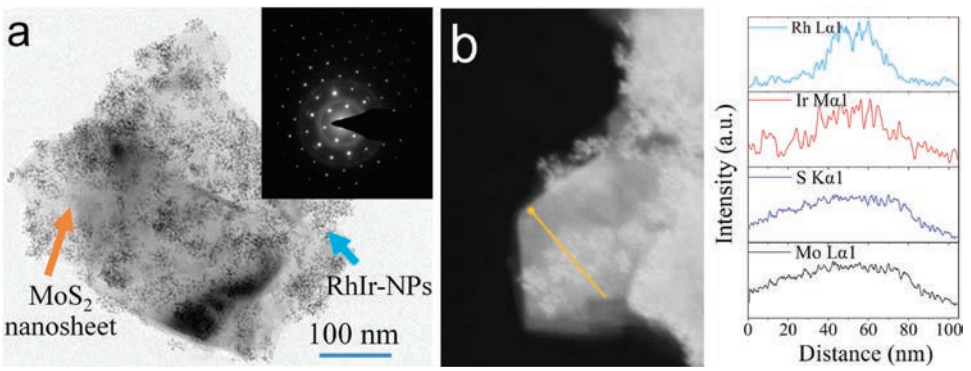

Fig. 1. Characterizations of RhIr@MoS_2 nanohybrids. (a) TEM image and SAED image (inset), (b) STEM image and the corresponding elemental line profiles of RhIr@MoS_2.

Since RhIr@MoS_2 nanohybrid is an integrated structure, each of its components may possess different functions and exert diverse effects during electrochemical sensing process. Firstly, electrochemical impedance measurement is carried out to study the transport/diffusion ability of RhIr@MoS_2 nanohybrids modified microsensor. Generally, the depressed semicircle in high frequency is related to the electron transfer resistance (R_{ct}), while the straight line at low frequency is in correlation with the diffusion process at the electrode surface [26]. Fig. 3 shows the Nyquist plots of RhIr@MoS_2 nanohybrids based microsensor, and the measurements on MoS_2 based microsensor and blank microsensor are also conducted for comparison. Obviously, the electrochemical impedance spectroscopy (EIS) of blank microsensor displays a deformed semicircle, while the semicircle is almost disappeared when MoS_2 or RhIr@MoS_2 is introduced onto the electrode. The above results indicate that both electron transfer and diffusion-controlled process over blank microsensor has been altered to a typical diffusion-controlled process arising from modified microsensor. In addition, the diffusion process is facilitated by RhIr nanocrystals which could be revealed from the slop comparison of EIS curves at low frequency. Accordingly, the introduction of ultra-thin 2D MoS_2 into microsensor system could accelerate the electron transfer at electrode interface, and then the mass diffusion becomes the control step of reaction rate. Moreover, integrating RhIr nanocrystals on MoS_2 surface can further speed up the diffusion process of electrochemical reaction. Therefore, it can be expected that RhIr@MoS_2 nanohybrids are suitable for acting as sensing material for the detection of NADH.

Representative cyclic voltammogram (CV) response of RhIr@MoS_2 modified microsensor is firstly measured, and curves recorded within 500 nmol/L and 1 μmol/L of NADH are depicted in Fig. S2a (Supporting information). From the comparison with background, the obvious oxidation current is generated for both CV curves with the addition of 1 μmol/L and 500 nmol/L NADH, and an apparent oxidation peak at 0.07 V is observed. Such a low oxidation potential implies that the fabricated microsensor has a considerable capability to electrocatalytically oxidize NADH. The CV responses of blank microsensor towards the same concentration of NADH are also evaluated for comparison (Fig. S2b in Supporting information). About 100 times higher current response is produced by RhIr@MoS_2 nanohybrids modified microsensor compared with blank microsensor, and no obvious oxidation peak is generated over blank microsensor.

For assessment the sensitivity of the fabricated microsensor, amperometric measurements at applied potential of 0.07 V are performed for different NADH concentration detection in both μmol/L and nmol/L ranges. From Fig. S2c (Supporting information), the linear current increase is produced in the concentration of 1–20 μmol/L and the coefficient of determination (R^2) is estimated as 0.9739. Fig. S2d (Supporting information) displays the amperometric responses of RhIr@MoS_2 nanohybrids based microsensor sensing towards 5–100 nmol/L of NADH. The changed linear relationship between μmol/L and nmol/L ranges could be ascribed to the variation of mass transfer in different concentration ranges.

The differential pulse voltammetry (DPV) responses of NADH in bovine serum albumin (BSA) buffer solution also have been evaluated, and the results are shown in Fig. 4a. The background response in BSA buffer solution is quite close to the response in PBS solution, and almost overlaps with each other. With continuing detection of different NADH concentrations in BSA solution, a series of distinctive peaks are shown in the DPV measurements. Notably, the ultra-low detection limit of 1 nmol/L NADH in BSA buffer solution is obtained over the fabricated microsensor. We have also compared our results with previous reports [27–31], and the detailed comparison parameters are shown in Table S1 (Supporting information). Taking into consideration from either applied potential or detection limit for NADH determination, the explored RhIr@MoS_2 nanohybrids based microsensor achieves a comparative sensing performance. In addition, our developed microsensor also possesses a good anti-interference capability in the relatively complex BSA environment. The detection technique also performs a good repeatability as shown in Fig. 4b. After evaluation the DPV responses of seven fabricated microsensors towards 1 nmol/L NADH in BSA buffer solution, the standard deviation is obtained as 11.62.

The practical applicability of developed RhIr@MoS_2 nanohybrids based microsensor is finally demonstrated by analyzing NADH in real human serum samples. A total of 40 samples are tested, including 22 samples from cancer patients and 18 samples from cancer-free individuals. And each of the measurements is repeated three times to ensure the accuracy of results. As shown in Fig. 4c, the NADH oxidation current generated from cancerous cases is lower than that from noncancerous cases, which is consistent with previous reports [32,33]. Among the 22 cancerous cases, 5 of them produce the unusually high signals, and 2 of 18 noncancerous samples display the abnormal expression. According to the test results, the diagnosis sensitivity of 77.3% and specificity of 88.9% are acquired. From the sensing performance evaluation to real human samples assay, the developed RhIr@MoS_2 nanohybrids based microsensor show the superiority in terms of sensitivity, specificity and detection limit, illustrating that this developed

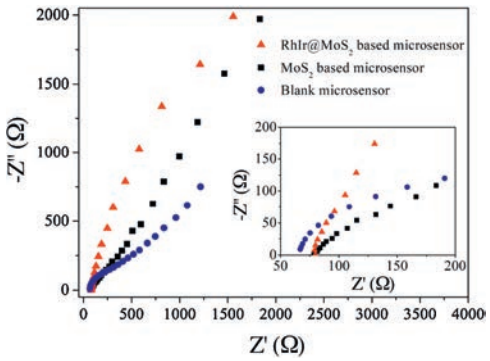

Fig. 3. Nyquist plots of blank microsensor, MoS_2 modified microsensor and RhIr@MoS_2 modified microsensor.

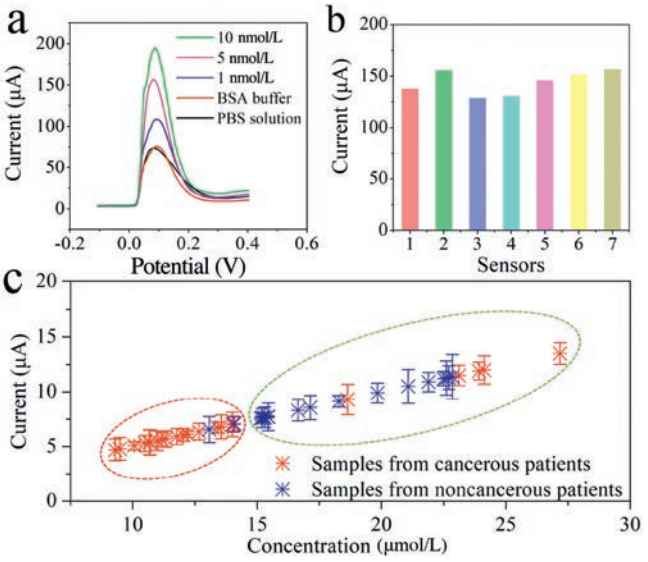

Fig. 4. (a) DPV measurements in BSA buffer solution, (b) repeatability evaluation, (c) testing results of real human serum samples from cancer patients and cancer-free individuals.

detection technique is promising for measuring NADH in biological fluids obtained from cancer patients.

In summary, RhIr alloy nanocrystals are successfully *in-situ* grown on the surface of 2D MoS_2 nanomaterial, and are used as sensing material for the distinct detection of NADH. With local deposition onto electrochemical microsensor, RhIr@MoS_2 nanohybrids possess the ability to detect NADH at an ultra-low potential of 0.07 V. Amperometric detections demonstrate that a considerable response is obtained in both nmol/L and μmol/L ranges. And the detection limit is evaluated as 1 nmol/L even in the complex BSA buffer environment. In addition, the real human serum samples assay shows that 17 of 22 cancerous cases display the low expression for NADH and 16 of 18 noncancerous samples reveal the normally high expression for NADH. The favorable performance of developed microsensor could be attributed to the assembled nanohybrid, which can not only provide the effective transportation channels for detective molecules, but also allows to specifically identifying NADH in body fluids.

Declaration of competing interest

The authors declare no conflict of interests.

Acknowledgments

This research is supported by National Key R&D Program of China (No. 2016YFA0200800), Shanghai Science and Technology Innovation Action Plan (No. 19520744200) and Natural Science Foundation of Shanghai (Nos. 17ZR1410000, 18ZR1415400). Y.Z. appreciates the financial support of State Key Laboratory of Transducer Technology of China (No. SKT1806).

Appendix A. Supplementary data

Supplementary material related to this article can be found, in the online version, at doi:https://doi.org/10.1016/j.cclet.2019.12.029.

References

[1] Y.Z. Zhao, J. Jin, Q.X. Hu, et al., Cell Metab. 14 (2011) 555–566.
[2] Y.Z. Zhao, Q.X. Hu, F.X. Cheng, et al., Cell Metab. 21 (2015) 777–789.
[3] H. Wang, Z. Gao, X.Y. Liu, et al., Nat. Commun. 9 (2018) 562.
[4] Q. Chen, C. Liang, X.Q. Sun, et al., PNAS 114 (2017) 5343–5348.
[5] L.L. Zhu, Y. Zhang, P.C. Xu, et al., Biosens. Bioelectron. 80 (2016) 601–606.
[6] W. Li, X.Y. Gong, X.P. Fan, et al., Chin. Chem. Lett. 30 (2019) 1775–1790.
[7] L. He, Y. Li, Q. Wu, et al., ACS Appl. Mater. Interfaces 11 (2019) 29158–29166.
[8] Y.H. Zhao, K.Y. Wei, F.P. Kong, et al., Anal. Chem. 91 (2019) 1368–1374.
[9] Y. Mie, Y. Yasutake, M. Ikegami, M. Ikegami, T. Tamura, Sens. Actuator. B -Chem. 288 (2019) 512–518.
[10] S. Teanphonkrang, S. Janke, P. Chaiyen, et al., Anal. Chem. 90 (2018) 5703–5711.
[11] P.H. Ling, Q. Zhang, T.T. Cao, F. Gao, Angew Chem. Int. Ed. 57 (2018) 6819–6824.
[12] W.J. Qin, C.C. Xu, Y.F. Zhao, et al., Chin. Chem. Lett. 29 (2018) 1451–1455.
[13] R.K. Tao, Y.Z. Zhao, H.Y. Chu, et al., Nat. Methods 14 (2017) 720–728.
[14] W. Zhang, R.G. Wang, F. Luo, P.L. Wang, Z.Y. Lin, Chin. Chem. Lett. (2019), doi: http://dx.doi.org/10.1016/j.cclet.2019.09.022.
[15] A. Dhiman, P. Kaira, V. Bansal, J.G. Bruno, T.K. Sharma, Sens. Actuator. B -Chem. 246 (2017) 535–553.
[16] W. Gao, S. Emaminejad, H.Y.Y. Nyein, et al., Nature 529 (2016) 509–514.
[17] Y.W. Li, Y. Chen, Y.H. Ma, et al., Chin. J. Anal. Chem. 42 (2014) 759–765.
[18] F.S. Omar, N. Duraisamy, K. Ramesh, S. Ramesh, Biosens. Bioelectron. 79 (2016) 763–775.
[19] H.W. Hu, A. Zavabeti, H.Y. Quan, et al., Biosens. Bioelectron. 142 (2019) 111573.
[20] V. Yadav, S. Roy, P. Singh, Z. Khan, A. Jaiswal, Small 15 (2019) 1803706.
[21] A. Sinha, Dhanjai, B. Tan, et al., TrAC-Trend Anal. Chem. 102 (2018) 75–90.
[22] Q. Fu, X.H. Bao, Chem. Soc. Rev. 46 (2017) 1842–1874.
[23] N. Wongkaew, M. Simsek, C. Griesche, A.J. Baeumner, Chem. Rev. 119 (2019) 120–194.
[24] S. Hossain, Y. Niihori, L.V. Nair, et al., Acc. Chem. Res. 51 (2018) 3114–3124.
[25] C. Altavilla, M. Sarno, P. Ciambelli, Chem. Mater. 23 (2011) 3879–3885.
[26] R. Maalouf, C. Fournier-Wirth, J. Coste, et al., Anal. Chem. 79 (2007) 4879–4886.
[27] K. Selvarani, A. Prabhakaran, P. Arumugam, S. Berchmans, P. Nayak, Microchim. Acta 185 (2018) 411.
[28] V. Vukojevic, S. Djurdjic, M. Ognjanovic, et al., Biosens. Bioelectron. 117 (2018) 392–397.
[29] L. Blandon-Naranjo, F. Della Pelle, M.V. Vazquez, et al., Electroanal. 30 (2018) 509–516.
[30] N.F. Atta, S.A.A. Gawad, E.H. El-Ads, A.R.M. El-Gohary, A. Galal, Sens. Actuator. B -Chem. 251 (2017) 65–73.
[31] M. Thiruppathi, P.Y. Lin, Y.T. Chou, et al., Talanta 200 (2019) 450–457.
[32] F. Torabi, K. Ramanathan, P.O. Larsson, et al., Talanta 50 (1999) 787–797.
[33] M.C. Skala, K.M. Riching, A. Gendron-Fitzpatrick, et al., PNAS 104 (2007) 19494–19499.